Available online at www.sciencedirect.com
SCIENCE DIRECT
Journal of Solid State Chemistry 179 (2006) 1984–1989
JOURNAL OF SOLID STATE CHEMISTRY
www.elsevier.com/locate/jssc

Chemical growth of ZnO nanorod arrays on textured nanoparticle nanoribbons and its second-harmonic generation performance

Zhou Gui[a,*], Xian Wang[b], Jian Liu[c], Shanshan Yan[c], Yanyan Ding[a], Zhengzhou Wang[a], Yuan Hu[a]

[a]*State Key Lab of Fire Science, University of Science and Technology of China, Hefei 230027, PR China*
[b]*Department of Physics, Air Force Engineering University, Xian 710038, PR China*
[c]*Department of Chemistry, University of Science and Technology of China, Hefei 230027, PR China*

Received 2 January 2006; received in revised form 1 March 2006; accepted 23 March 2006
Available online 1 April 2006

Abstract

On the basis of the highly oriented ZnO nanoparticle nanoribbons as the growth seed layer (GSL) and solution growth technique, we have synthesized vertical ZnO nanorod arrays with high density over a large area and multi-teeth brush nanostructure, respectively, according to the density degree of the arrangement of nanoparticle nanoribbons GSL on the glass substrate. This controllable and convenient technique opens the possibility of creating nanostructured film for industrial fabrication and may represent a facile way to get similar structures of other compounds by using highly oriented GSL to promote the vertical arrays growth. The growth mechanism of the formation of the ordered nanorod arrays is also discussed. The second-order nonlinear optical coefficient d_{31} of the vertical ZnO nanorod arrays measured by the Maker fringes technique is 11.3 times as large as that of d_{36} KH_2PO_4 (KDP).

Keywords: ZnO; Nanorod arrays; Solution growth; Nanostructure

1. Introduction

Zinc oxide (ZnO) is a well-known semiconductor for its wide bandgap (3.37 eV) and high exciton binding energy of 60 meV at room temperature. As a consequence, it possesses unique optical, acoustical, and electronic properties which stimulate wide research interest in its potential applications [1,2]. A particularly striking recent observation is that of room-temperature lasing action in ZnO nanorod arrays [3], highlighting the prospects that the functional design of ZnO nanostructure in a highly oriented and an ordered array is of crucial importance for the development of a device in practical applications with high performance.

Vertically ZnO nanorod arrays can be grown by vapor-phase deposition methods on catalytically treated substrate [3,4] or on an epitaxial substrate such as sapphire [5]. However, growth techniques usually expensive, the choice of substrate restricted, complex process control and high temperature are unfavorable for an industrialized process. Recently, a solution-based approach was developed to achieve highly oriented nanorod film with high surface area on wafer, which has the advantages of mild synthetic conditions, simple manipulation and large scale-up production, and opens a door for future optoelectronic devices based on ZnO nanostructure arrays [6–10]. Generally, homogeneous nucleation of solid phases requires a higher activation energy barrier, and therefore, hetero-nucleation will be promoted and will be energetically more favorable (e.g., influence of seeding on crystal growth). Consequently, hetero-nucleation takes place at a lower saturation ratio onto a substrate than in homogeneous solution. Thus far, in this technique, the initial deposition of the growth seed layer (GSL) on a substrate is critical for the formation of the arrays of ZnO nanorods with high qualities [8,10]. The major problem in front of practical optoelectronic applications is to find appropriate intermediate layer,

*Corresponding author. Fax: +86 551 360 1669.
E-mail address: zgui@ustc.edu.cn (Z. Gui).

0022-4596/$ - see front matter © 2006 Elsevier Inc. All rights reserved.
doi:10.1016/j.jssc.2006.03.035

which is well adhered to the substrate and suitable for the following solution growth. To our knowledge until now, almost all the solution-based synthesis methods rely on precoating the substrate with a ZnO nanocrystal layer as the GSL prior to the actual solution-based synthesis [8–10]. ZnO nanocrystals were used to spin cast several times onto a substrate and several times annealing at 150 °C is necessary between coatings to ensure particle adhesion to the substrate surface [8].

Recently, we have demonstrated [11] that a new 1-D nanostructure, porous structured nanoribbons which are self-assembled by highly oriented ZnO nanoparticles (nanoparticle nanoribbons), was obtained upon removal of ligand molecules from a novel ribbonlike precursor $ZnO \cdot 0.15Zn(CH_3COO)_2 \cdot 0.85H_2O$. In the present work, we combine this highly oriented ZnO nanoparticle nanoribbons as the GSL with the solution growth approach to grow large-area high-density ordered arrays of aligned ZnO nanorods. Meanwhile, a three-dimensional (3D) multi-teeth brush nanostructure was also found under different growth conditions. The formation of the 3D nanostructure is helpful to further understand the mechanism of nanorod arrays growth in solution phase and proves that the highly oriented ZnO GSL are the director to grow ZnO nanorods with orientation and position controlled on it. The results of second-order nonlinear optical (NLO) measurements suggest the large NLO effects of ZnO nanorod arrays we have obtained and the potential application as optoelectronic nanodevice.

2. Experimental

The precursor nanoribbons were synthesized as we reported [11]. To prepare the precursor, 50 mL 0.1 M $Zn(CH_3COO)_2 \cdot 2H_2O$ and 50 mL 0.15 M $NH_2 \cdot NH_2$ was mixed, stirred for 30 min, then was heated at 40 °C for 4 h. After the precursor was centrifuged and dispersed in the acetone in adequate concentration, the precursor nanoribbons were then cast onto a glass substrate just once. To obtain highly oriented ZnO GSL, the substrate was dried and annealed at 500 °C for 3 h in air conditions. After coating the glass substrate with ZnO nanoparticle nanoribbons GSL, the vertical ZnO nanorod arrays growth was carried out by suspending the substrate upside-down in an open dish filled with an aqueous solution of zinc nitrate (0.1 M) and methenamine [6,8] (0.1 M) at 90 °C for 3 h. The substrate was then removed from solution, rinsed with deionized water, and dried.

X-ray powder diffraction (XRD) analysis was conducted out on a Rigaku D/Max X-ray diffractometer with graphite monochromated Cu$K\alpha$ radiation ($\lambda = 1.5418$ Å). Scanning electron microscopy (SEM) images were recorded on a JSM-6700F scanning electron microscope, working at 100 KeV acceleration voltages.

The coefficient d_{31} of ZnO nanorod arrays with the height of 2.60 μm can be measured independently with the Maker fringes technique [12–14]. The calibration is the conventional KH_2PO_4 (KDP) crystal. The incident fundamental wave 1064 nm was parallel to the rotating axis (*a*-axis), which was emitted by Q-Switched Nd:YAG nanosecond pulsed laser with repetition 10 Hz. The transmitted second-harmonic wave, 532 nm, was perpendicular to the *a*-axis, was detected by the photomultiplier and collected by Boxcar.

3. Results and discussion

After the acetone solution was vaporized, the substrate was heated at 500 °C for 3 h in air condition, and then the highly oriented ZnO GSL is formed on the substrate. Fig. 1a is the typical XRD pattern of ZnO GSL on a glass substrate. The 0 0 2 reflection has strongly sharpened up which shows the *c*-axis of most of the ZnO nanocrystals preferentially oriented perpendicular to the plane of the glass substrate. The highly oriented alignment of ZnO nanocrystals is substrate-independent and occurs on flat surfaces regardless of the characteristics of the substrate used. This orientation is probably due to an intrinsic thermodynamic feature of the growth of ZnO nuclei [15]. Such a coincidental matchup along the [001] direction, along with a strong tendency of ZnO to grow in the *c* orientation, more easily leads to the following unique vertical solution growth configuration [3].

Fig. 2 presents SEM images recorded from the ZnO nanorods arrays growth in zinc nitrate (0.1 M) and methenamine [6,8] (0.1 M) system solution at 90 °C for 3 h. Fig. 2a shows a top view of the ZnO nanorod arrays over a large area. The magnified images of the top view are shown in Fig. 2b and c. It is clear that well-aligned hexagonal rod arrays with high density ($2–4 \times 10^9$ cm^{-2}) grow along the [001] direction perpendicular to the

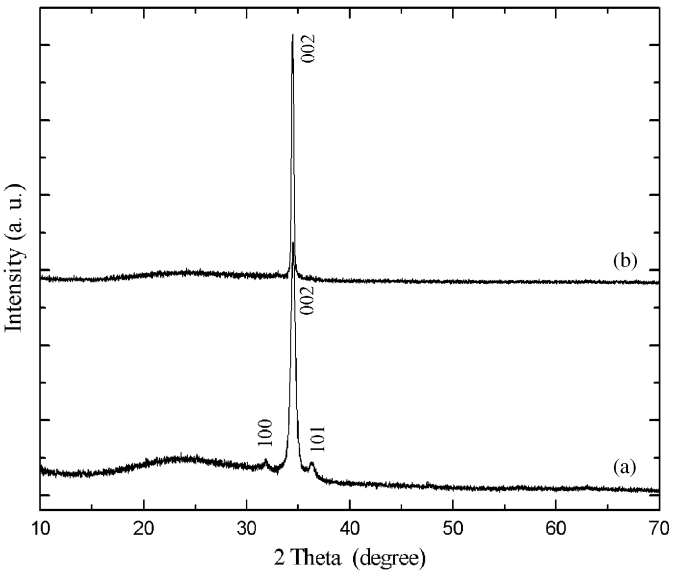

Fig. 1. Powder X-ray diffraction patterns of (a) highly oriented nanoparticle nanoribbons ZnO GSL on a glass substrate and (b) ZnO nanorod arrays grown on the GSL.

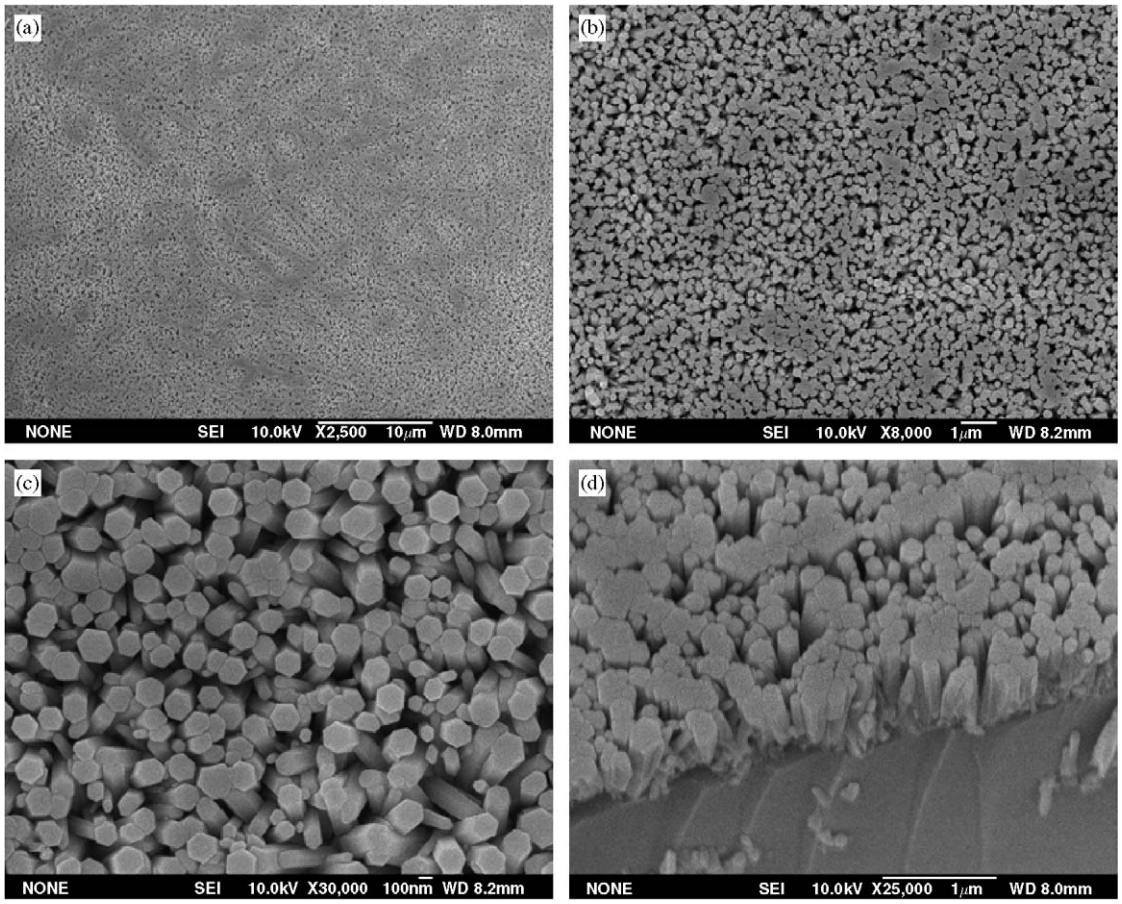

Fig. 2. SEM images of the arrays at different locations and magnifications. These images are representatives of the entire surface.

substrate. Perfect hexagonal end planes and well-faceted side surfaces of the rods are clearly identified. The hexagonal arrangement of the aligned ZnO nanorods can be clearly distinguished in the magnified image of a 20° side view shown in Fig. 2d. All of the ZnO nanorods have about the same height, of about 2.6 μm and their diameters range between 50 and 150 nm. The [001] preferential nanorod growth on the glass substrate is also reflected in the XRD pattern (Fig. 1b). Only (002) peak is observed, indicating excellent overall *c*-axis alignment of these nanorods arrays over a large substrate area [9,10,15–20]. Although there have been many attempts to achieve an orientation control grown ZnO nanorod arrays on different substrates through soft solution processes, their (001) XRD intensities appeared to be fairly weak and many (*hk*0) peaks were observed due to the random orientation of ZnO nanorods [6,9,15].

An interesting 3D-long multi-teeth brush structure is also found on the substrate area with sparse nanoparticle nanoribbons ZnO GSL (Fig. 3), when the concentration of growth solution was reduced to 0.025 M, keeping other experimental variables unchanged. All the ZnO nanorods grow vertically and regularly on the GSL nanoribbons, even on the nanoribbon splits (Fig. 3c). Almost no nanorods were observed to grow along the ribbon lateral direction, which is different to that of the reports via the vapor–liquid–solid (VLS) method [21,22]. It is indicated that the order and the regular ZnO nanorod arrays can be growth controlled by solution conditions. From Fig. 3b and c, at the cross junctions of nanoribbons, the nanorods grow very well and have no difference to that of the other area on the ribbons. The results are favorable since high-quality ordered nanorod arrays over a large area could be obtained with dense nanoparticle nanoribbons as the GSL (Fig. 2).

The formation of the long multi-teeth brush nanostructure is helpful to study the growth mechanism of large-scale ordered vertical arrays. It is clear that ZnO nanorods grow vertically only on the region that was coated with ZnO nanoparticle nanoribbons, no ZnO nanorods are found on the spacing area where glass was exposed because the ZnO GLS may lower the lattice mismatch between the deposition and the substrate [19]. The growth mechanism of large-scale vertical arrays on GSL in a large area is determined by the growth method of nanorods on a single nanoparticle nanoribbon in nanoscale. Single-crystalline ZnO nanorods synthesized always grow along the *c*-axis direction regardless of the growth method [15], which suggests that the *c*-axis is the fastest growth direction and therefore that ZnO {001} is of the highest energy of the

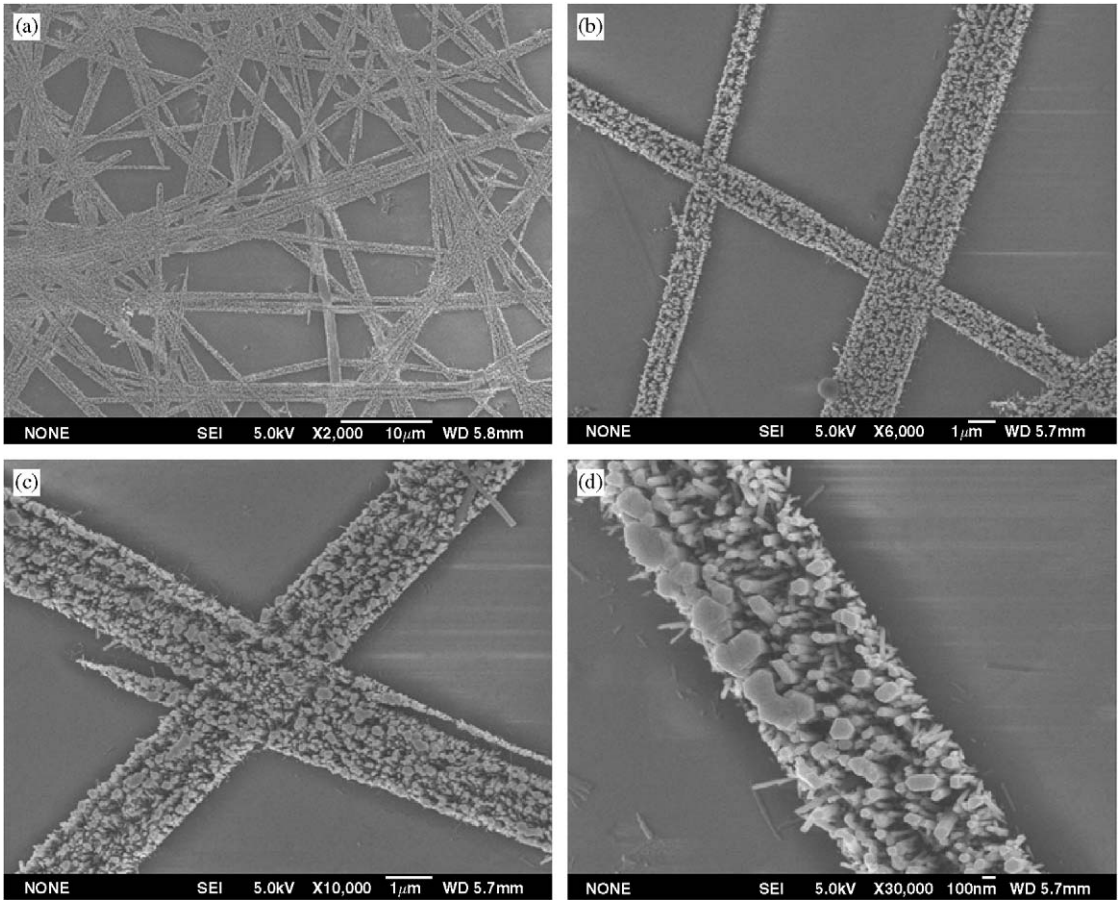

Fig. 3. SEM images of 3D long multi-teeth brush nanostructure at different locations and magnifications in the lower concentration growth solution.

low-index surfaces. Although crystal growth in any direction occurs at the nucleation on the surface, the preferential direction growth along the *c*-axis would be dominant on the textured ZnO nanoparticles as the crystal growth proceeds. The competing facet's growth is constrained by the fastest growth. Our XRD patterns results (Fig. 1) of the synthesized nanorod arrays also demonstrate that the orientation of the ZnO GSL directly determines the orientation of the nanorods.

When the concentration of growth solution is as higher as 0.1 M, the morphology (Fig. 4) of the nanorods growth on a single nanoparticle nanoribbon is different to that (Fig. 3d) in lower concentration. The diffusion rate of the growing units and the crystal growth rate at the liquid–solid interface are relatively fast in higher concentration. In the result, the rods growth in the lateral direction can be found. This growth phenomenon is also found in aligned growth of ZnO nanorods via VLS method [10,13,14]. In fact, this microstructure growth mode has no effect on the growth of oriented vertical nanorod arrays (Fig. 2) in higher concentration growth solution. As the crystal growth proceeds, the preferential growth along the *c*-axis would be maintained. Along with the vertical rods growth that is long and dense, the lateral growth is constrained by contact between adjacent vertical rods. Based on a series of experiments, we find that the height of the arrays and the average size of the nanorods increase with higher concentration growth solution or longer reaction time.

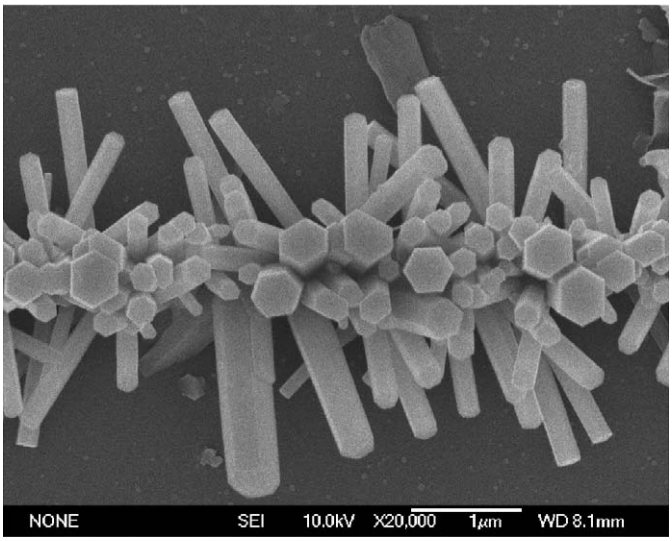

Fig. 4. SEM image of 3D ZnO nanorods nanostructure in the higher concentration growth solution.

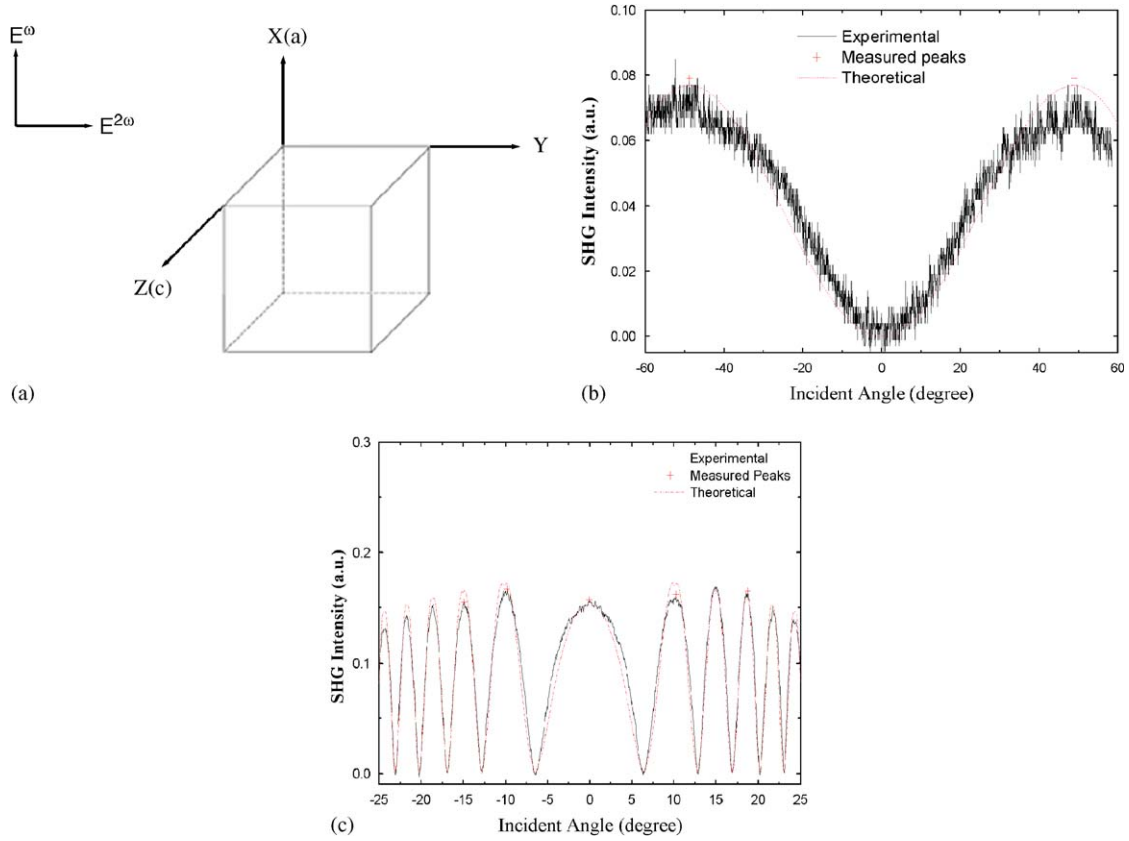

Fig. 5. (a) Schematic presentation of the measurement of the NLO efficiency, the Maker fringes of (b) d_{31} of vertical ZnO nanorod arrays and (c) d_{36} of the KDP crystal. The solid curve represents the experimental fringes, and the dashed curve the theoretical fringes.

According to the structure of the ZnO nanorods, which belongs to a hexagonal, non-centrosymmetric space group $P63mc$, the vertical ZnO nanorods arrays should have the second-harmonic efficiency and the non-zero second-order NLO efficiency. Nevertheless, the NLO properties of the vertical nanorods arrays are scarcely explored. During the experiment, the measurements are schematized in Fig. 5a. The experimental Maker fringe of the coefficient d_{31} of ZnO nanorods arrays is shown as the solid curve of Fig. 5b. Similarly, the Maker fringe of d_{36} (KDP) is measured as Fig. 5c.

The Maker fringe technique [12–14] is a method to measure second-order NLO coefficients of the sample relative to the calibration. According to the Maker fringe theory, the transmitted second-harmonic power, $P_{2\omega}(\theta)$, which depicts the Maker fringe, is given by

$$P_{2\omega} = \frac{512\pi^2 d^2}{cr^2} P_{\mathrm{M}}(\theta)\sin^2\psi = aP_{\mathrm{M}}(\theta)\sin^2\psi, \quad (1)$$

$$\psi = \frac{\pi L}{2}\frac{4}{\lambda}(n_{1\omega}\cos\theta_{1\omega} - n_{2\omega}\cos\theta_{2\omega}), \quad (2)$$

where θ is the external rotating angle, d the second-harmonic coefficient, c the light speed in the vacuum, r the radius of the laser beam, $a = 512\pi^2 d^2/(cr^2)$. $P_{\mathrm{M}}(\theta)$ is the function of the angle θ and the fundamental wave power, L the thickness of the crystals, λ the fundamental wavelength, $n_{1\omega}$ and $n_{2\omega}$ the refractive indices at the fundamental and harmonic waves, $\theta_{1\omega}$ and $\theta_{2\omega}$ the refractive angles, respectively. Therefore, the magnitude of the second-order NLO coefficient is determined, as following:

$$\frac{\mathrm{d}^2_{ij(\mathrm{sample})}}{\mathrm{d}^2_{ij(\mathrm{calibration})}} = \frac{P_{2\omega}(\theta)_{\mathrm{sample}}}{P_{2\omega}(\theta)_{\mathrm{calibration}}}. \quad (3)$$

Then the NLO coefficient d_{31} of ZnO nanorods arrays is calculated as 11.3 times as large as d_{36} of the KDP crystal. Moreover, the dashed theoretical fitting fringes of ZnO and KDP can be drawn with Eq. (1), respectively. It is found that the experimental fringes agree well with the theoretical ones.

4. Conclusions

We have successfully synthesized ZnO nanorod arrays with high density over a large area by using highly oriented ZnO nanoparticle nanoribbons as the GSL in an aqueous solution. There are three advantages by using the new GSL: (i) the ordered nanorods arrays or the 3D nanostructure are obtained by controlling the density of the arrangement of nanoparticle nanoribbons, (ii) it is just needed to coat the precursor GSL on a substrate for one time by controlling the precursor concentration, which is convenient for future industrial production, (iii) the results

of the second-order NLO measurements suggest the large NLO effects of ZnO nanorod arrays we have obtained and the potential application of them as optoelectronic nanodevices. Furthermore, the formation of ZnO nanorod arrays by using highly oriented GSL to promote the vertical arrays growth may represent a facile way to get similar structures of other compounds.

Acknowledgments

This work was financially supported by the National Natural Foundation of China (No. 20571070) and the special foundation of State Key Lab of Fire Science.

References

[1] Y. Xia, P. Yang, Y. Sun, Y. Wu, B. Mayers, B. Gates, Y. Yin, F. Kim, H. Yan, Adv. Mater. 15 (2003) 353.
[2] M. Hiramatsu, K. Imaeda, N. Horio, M. Nawata, J. Vac. Sci. Technol. A 16 (1998) 669.
[3] M.H. Huang, S. Mao, H. Feick, H. Yan, Y. Wu, H. Kind, E. Weber, R. Russo, P. Yang, Science 292 (2001) 1897.
[4] P.X. Gao, Y. Ding, Z.L. Wang, Nano Lett. 3 (2003) 1315.
[5] W.I. Park, D.H. Kim, S.W. Jung, G. Yi, Appl. Phys. Lett. 80 (2002) 4232.
[6] L. Vayssieres, Adv. Mater. 15 (2003) 464.
[7] L. Vayssieres, K. Keis, A. Hagfeldt, S. Lindquist, Chem. Mater. 13 (2001) 4395.
[8] L.E. Greene, M. Law, J. Goldberger, F. Kim, J.C. Johnson, Y. Zhang, R.J. Saykally, P. Yang, Angew. Chem. Int. Ed. 42 (2003) 3031.
[9] J. Choy, E. Jang, J. Won, J. Chung, D. Jang, Y. Kim, Adv. Mater. 15 (2003) 1911.
[10] K. Govender, D. Boyle, P. Kenway, P. O'Brien, J. Mater. Chem. 14 (2004) 2575.
[11] Z. Gui, J. Liu, Z. Wang, L. Song, Y. Hu, W. Fan, D. Chen, J. Phys. Chem. B 109 (2005) 1113.
[12] P.D. Maker, R.W. Terhune, M. Nisenoff, C.M. Savage, Phys. Rev. Lett. 8 (1962) 21.
[13] J. Jerphergon, S. Kurtz, Phys. Rev. B 1 (1970) 1739.
[14] J. Jerphergon, S. Kurtz, J. Appl. Phys. 41 (1970) 1667.
[15] L. Greene, M. Law, D. Tan, M. Montano, J. Goldberger, G. Somorjai, P. Yang, Nano Lett. 5 (2005) 1231.
[16] Q. Tang, W. Zhou, J. Shen, W. Zhang, L. Kong, Y. Qian, Chem. Commun. (2004) 712.
[17] H. Zhang, X. Sun, R. Wang, D. Yu, J. Cryst. Growth 263 (2004) 119.
[18] Y. Koh, M. Lin, C. Tan, Y. Foo, K. Loh, J. Phys. Chem. B 108 (2004) 11419.
[19] H. Yu, Z. Zhang, M. Han, X. Hao, F. Zhu, J. Am. Chem. Soc. 127 (2005) 2378.
[20] J. Hsu, Z. Tian, N. Simmons, C. Matzke, J. Voigt, J. Liu, Nano Lett. 5 (2005) 83.
[21] M. Huang, Y. Wu, H. Feick, N. Tran, E. Weber, P. Yang, Adv. Mater. 13 (2001) 113.
[22] P.X. Gao, Z.L. Wang, J. Phys. Chem. B 18 (2004) 7534.